The Journal of Immunology

RESEARCH ARTICLE | AUGUST 15 2013

Differential Regulation of TLR-Dependent MyD88 and TRIF Signaling Pathways by Free Zinc Ions FREE

Anne Brieger; ... et. al

J Immunol (2013) 191 (4): 1808–1817.
https://doi.org/10.4049/jimmunol.1301261

Differential Regulation of TLR-Dependent MyD88 and TRIF Signaling Pathways by Free Zinc Ions

Anne Brieger, Lothar Rink, and Hajo Haase

Zinc signals are utilized by several immune cell receptors. One is TLR4, which causes an increase of free zinc ions (Zn^{2+}) that is required for the MyD88-dependent expression of inflammatory cytokines. This study investigates the role of Zn^{2+} on Toll/IL-1R domain–containing adapter inducing IFN-β (TRIF)–dependent signals, the other major intracellular pathway activated by TLR4. Chelation of Zn^{2+} with the membrane-permeable chelator N,N,N',N'-Tetrakis(2-pyridylmethyl)ethylenediamine augmented TLR4-mediated production of IFN-β and subsequent synthesis of inducible NO synthase and production of NO. The effect is based on Zn^{2+} acting as a negative regulator of the TRIF pathway via reducing IFN regulatory factor 3 activation. This was also observed with TLR3, the only TLR that signals exclusively via TRIF, but not MyD88, and does not trigger a zinc signal. In contrast, IFN-γ–induced NO production was unaffected by N,N,N',N'-Tetrakis(2-pyridylmethyl)ethylenediamine. Taken together, Zn^{2+} is specifically involved in TLR signaling, where it differentially regulates MyD88 and TRIF signaling via a zinc signal or via basal Zn^{2+} levels, respectively. ***The Journal of Immunology*****, 2013, 191: 1808–1817.**

The essential trace element zinc is indispensable for the function of the immune system. Zinc deficiency leads to increased susceptibility to infections, and restoring zinc levels of marginally deficient elderly by supplementation can improve immune function (1, 2). In recent years, it has become clear that the importance of zinc for immunity is based, at least in part, on a function in signal transduction in cells of the immune system (3). Intracellular zinc concentrations are tightly regulated by zinc transporters and zinc signals (4). The latter consists of a change in the cytoplasmic concentration of free zinc ions (Zn^{2+}), which have already been observed in response to several stimuli and in many different types of immune cells. In monocytes, MCP-1 (5), PMA (6), TNF-α, insulin, and the TLR ligands Pam3CSK4 and LPS (7) induce an intracellular increase of the cytosolic free Zn^{2+} concentration.

TLRs are a subgroup of the pattern-recognition receptors, which detect conserved molecular structures of pathogens that are used as danger signals by certain immune cells (8). Ligand binding to the ectodomain of TLRs induces dimerization, bringing their cytoplasmic Toll/IL-1R domains together, resulting in the recruitment of intracellular adapter proteins and initiation of downstream signaling events (9). TLR4 initially binds the adaptors TIRAP and MyD88, and causes phosphorylation of MAPKs and early activation of NF-κB. The zinc signal is required for preventing dephosphorylation of MAPKs p38, MEK1/2, and ERK1/2, and for NF-κB activation, and thereby for transcription and release of inflammatory cytokines, such as TNF-α, IL-1β, and IL-6 (7).

After activation of the MyD88-dependent pathway, the receptor complex is endocytosed (10) and the adaptors TRAM and Toll/IL-1R domain–containing adapter inducing IFN-β (TRIF) bind to TLR4, resulting in a delayed NF-κB signal and activation of the IFN regulatory factor 3 (IRF3) (11). Signaling via TRIF and IRF3 triggers the secretion of IFN-β (12). IFN-β binds to the type 1 IFNR, which, in turn, activates a JAK-STAT pathway inducing the expression of surface molecules required for the interaction with T cells, such as CD40, CD80, and CD86 (13, 14). Together, the activation of NF-κB and JAK-STAT also induces the expression of inducible nitric monoxide synthase (iNOS) (15–17). iNOS activity is mainly regulated through gene expression, and its product NO is an important mediator of inflammation (18). Functions of iNOS-derived NO are the elimination of microbes, parasites, and cancer cells (18, 19).

Still, it is poorly understood how the TLR-induced inflammatory and antiviral immune responses are balanced. Zinc signals affect the TLR4-induced production of MyD88-dependent inflammatory cytokines (7), and the aim of this study is to investigate whether intracellular Zn^{2+} levels also affect the TLR4-induced activation of the TRIF pathway, in particular, the release of the inflammatory mediator NO.

Materials and Methods

Cell culture

All cell lines were cultured at 37°C in a humidified 5% CO_2 atmosphere. RAW 264.7 murine macrophages, L929 fibroblasts, and 7FD3 hybridoma cells were grown in RPMI 1640 (Lonza, Verviers, Belgium) containing 10% FCS (heat inactivated for 30 min at 56°C; PAA, Cölbe, Germany), 2 mM L-glutamine, 100 U/ml potassium penicillin, and 100 U/ml streptomycin sulfate (all from Lonza). 3T3 and 293T cells were grown in DMEM (Lonza) supplemented as described earlier. Zinc-deficient medium was obtained by treatment with CHELEX 100 ion exchange resin (Sigma-Aldrich, St. Louis, MO) as described previously (20).

Bone marrow–derived macrophages

Bone marrow was isolated from the femurs of C57BL/6 mice. A total of 3×10^5 cells/ml was seeded in 20 ml RPMI 1640 containing 18% heat-inactivated FCS, 2 mM L-glutamine, 100 U/ml potassium penicillin, 100 U/ml streptomycin sulfate, 1 mM nonessential amino acids (Lonza), and

Institute of Immunology, Medical Faculty, RWTH Aachen University, 52074 Aachen, Germany

Received for publication May 13, 2013. Accepted for publication June 13, 2013.

This work was supported by German Research Council (Deutsche Forschungsgemeinschaft) Grant HA4318/3 (to H.H.).

Address correspondence and reprint requests to Prof. Hajo Haase, Institute of Immunology, Medical Faculty, RWTH Aachen University, Pauwelsstrasse 30, 52074 Aachen, Germany. E-mail address: HHaase@ukaachen.de

The online version of this article contains supplemental material.

Abbreviations used in this article: BMM, bone marrow–derived macrophage; iNOS, inducible nitric monoxide synthase; IRF3, IFN regulatory factor 3; PTP, protein tyrosine phosphatase; TPEN, N,N,N',N'-Tetrakis(2-pyridylmethyl)ethylenediamine; TRIF, Toll/IL-1R domain–containing adapter inducing IFN-β.

20% sterile-filtered L929 cell culture supernatant for a total of 8 d. On day 4, 10 ml fresh culture medium was added. On day 7, the medium was completely replaced. On the next day, experiments were performed.

Production of IFN-β–containing cell-free culture supernatant

The supernatants of 3T3 and 293T cells stably transfected to produce mouse IFN-β were collected 4 d after seeding and were centrifuged for 10 min at 300 × *g*. Supernatants were sterile-filtered with a 0.22-μm filter (Millex-GV; Millipore, Billerica, MA), and aliquots were stored at −80°C until use. The activities of the IFN-β–containing cell supernatants were determined by an IFN-β bioassay with the L929 cell line and the *Encephalomyocarditis virus*. For all experiments, 2000 U/ml IFN-β was applied.

Purification of monoclonal anti–IFN-β Abs

7FD3 hybridoma cells produce rat IgG1 anti-mouse IFN-β Abs. The cells were grown for 3–4 d under normal culture conditions until confluency and cultured for 3 more days in serum-free medium (21). Supernatants were collected, sterile-filtered, and concentrated (Minicon B15 clinical sample concentrator; Millipore). The Ab was purified using an IgG Purification Kit (Pierce, Thermo Scientific, Rockford, IL) following the manufacturer's instructions and quantified using an IgG-Standard with a Bradford assay (Bio-Rad Laboratories). The purified Ab solution was sterile-filtered with a 0.22-μm filter (Millex-GV; Millipore), and 0.01–1 μg/ml of the Abs applied as depicted in Fig. 5C.

Zn^{2+} measurements with fluorescent probes

Cells were grown on a 96-well plate and incubated in loading buffer (25 mM HEPES [pH 7.35], 120 mM NaCl, 5.4 mM KCl, 5 mM glucose, 1.3 mM $CaCl_2$, 1 mM $MgCl_2$, 1 mM NaH_2PO_4, 0.3% BSA) for 30 min with 1 μM FluoZin-3-AM (Invitrogen, Eugene, OR) at 37°C. Subsequently, cells were washed twice with measurement buffer (incubation buffer without BSA). The resulting fluorescence was recorded on a Tecan Ultra 384 fluorescence well plate reader (Tecan, Crailsheim, Germany) using an excitation wavelength of 485 nm and measuring the emission at 535 nm. Intracellular free Zn^{2+} concentrations were calculated as previously described (6), using 50 μM N,N,N',N'-Tetrakis(2-pyridylmethyl)ethylenediamine (TPEN; Sigma-Aldrich) to determine minimal and 100 μM $ZnSO_4$/50 μM pyrithione to determine maximal fluorescence, respectively. TLR ligands were purchased from Invivogen (San Diego, CA).

Western blotting

A total of 5 × 10^5 cells was collected by centrifugation, lysed by sonication in 100 μl sample buffer (62.5 mM Tris-HCl [pH 6.8], 2% [w/v] SDS, 27% [v/v] glycerol, 0.1% [v/v] 2-ME, 0.01% [w/v] bromophenol blue, 1 mM Na_3VO_4), and heated for 3 min at 95°C. An equivalent of 1 × 10^5 cells/lane was separated on 10 or 14% (H3) polyacrylamide gels at 150 V and blotted to nitrocellulose membranes. Uniform loading of gels was confirmed by staining with Ponceau S. After destaining, membranes were blocked overnight with TBST (20 mM Tris-HCl [pH 7.6], 136 mM NaCl, 0.1% [v/v] Tween 20) containing 5% fat-free dry milk and incubated with the primary Abs at 1/1000 (anti-H3 1/20,000) dilution in TBST containing 5% BSA for 3 h. All primary Abs were purchased from Cell Signaling Technology with the exception of anti-H3 (Abcam, Cambridge, U.K.), anti-TRAF3, and anti–NF-κB (Santa Cruz Biotechnology). Membranes were washed three times with TBST and incubated for 1 h with goat anti-rabbit–HRP (Cell Signaling Technology) followed by detection with LumiGlo Reagent (Cell Signaling Technology) on an LAS-3000 (Fujifilm Lifescience, Düsseldorf, Germany). Densitometric quantification was performed with Adobe Photoshop Elements.

Nuclear extraction for Western blot samples

A total of 5 × 10^6 cells was thoroughly suspended in 2 ml ice-cold buffer (10 mM Tris-HCl, pH 7.4, containing 15 mM NaCl, 60 mM KCl, 0.5% Igepal CA-630, 1 mM EDTA, 0.1 mM EGTA) and lysed at 4°C for 5 min. Nuclei were pelleted by centrifugation (600 × *g*, 4°C, 5 min), taken up in 100-μl Western blot sample buffer, and treated as described earlier for Western blot samples.

RT-PCR

The mRNA of 5 × 10^5 cells was isolated after lysis in 1 ml Tri Reagent (Ambion, Life Technologies, Carlsbad, CA) and transcribed into cDNA with the qScript cDNA Synthesis Kit (Quanta Biosciences, Darmstadt, Germany) according to the manufacturers' instructions. Quantitative real-time PCR was performed on an ABI PRISM 7000 or a Step-One plus Real-Time PCR System (both from Applied Biosystems, Darmstadt, Germany) with the oligonucleotide sequences shown in Table I. The components of each PCR sample (final 25 μl) were 8 μl dH_2O, 12.5 μl Power SYBR-Green PCR MasterMix (Applied Biosystems), 1.25 μl forward and reverse primer each (2 μM), and 2 μl of the respective cDNA (50 ng/μl) or dH_2O as a negative control. The real-time PCR was performed in duplicate with the following parameters for iNOS and STAT1: 95°C for 15 min followed by 40 cycles of 95°C for 30 s and 58°C for 30 s; and for the other oligonucleotides: 95°C for 15 min followed by 40 cycles of 95°C for 30 s, 56°C for 1 min, and 72°C for 1 min. For quantification, the comparative cycle threshold method (ΔΔCT) was used, normalizing the results to the housekeeping gene β-actin.

Griess assay

Griess assay was performed modified after Griess (22). A total of 50 μl cell supernatant was incubated for 10 min with 50 μl of a 1% Sulfanilamide (Fluka, Sigma-Aldrich) solution in 5% phosphoric acid. A total of 50 μl of a 0.1% *N*-(1-naphtyl)ethylenediamine dihydrochloride (Riedel-de-Haën; Sigma-Aldrich) solution was added and incubated for 10 min. All samples were analyzed in duplicate. Nitrite production was determined by measuring the absorption at 520 nm in a Sunrise well plate reader (Tecan) and quantified with a standard curve from 0.78 to 50 μM nitrite.

Neutral red assay

Cellular viability was measured by neutral red uptake. RAW 264.7 cells (5 × 10^5 cells/ml) were grown for 24 h and treated for further 24 h with LPS and TPEN. Cells were loaded for 3 h with neutral red (final concentration, 55 μM), washed with PBS, lysed in a mixture of ethanol/H_2O/acetic acid (50:49:1), and neutral red uptake was quantified by its absorption at 540 nm in a Sunrise well plate reader (Tecan).

Flow cytometric measurement of endocytosis

TLR4 endocytosis was measured by flow cytometry as described previously (10). After incubation, RAW 264.7 cells were treated with anti-CD16/CD32 blocking Ab for 5 min in ice-cold PBS. Anti–TLR4-PE (clone MTS510) or PE-conjugated rat IgG2a,κ as isotype-matched control were added (all Abs were from BD Pharmingen, Heidelberg, Germany). Abs

Table I. Oligonucleotide sequences used for real-time PCR

Gene	Forward Primer	Reverse Primer
iNOS	5′-GGCAGCCTGTGAGACCTTTG-3′	5′-GCATTGGAAGTGAAGCGTTTC-3′
β-Actin (48)	5′-CGTGCGTGACATCAAAGAGA-3′	5′-CCATACCCAAGAAGGAAGGC-3′
Rantes	5′-CTCACCATCATCCTCACTGC-3′	5′-TCGAGTGACAAACACGACTG-3′
IP-10	5′-TGCCGTCATTTTCTGCCTC-3′	5′-TCGTGGCAATGATCTCAACA-3′
MCP-1	5′-TCAGCCAGATGCAGTTAACG-3′	5′-TCTGGACCCATTCCTTCTTG-3′
IFN-α	5′-AGTGATGAGCTACTGGTCAAC-3′	5′-TGATGCTGTGGAAGTATATCCT-3′
IFN-β	5′-CTCTCCATCAACTATAAGCA-3′	5′-CTTTCAAATGCAGTAGATTC-3′
CD40	5′-CCTTCTTCTTCTCACTAGAAA-3′	5′-ATTACAGATTTATTTAGCCAGT-3′
CD80	5′-CTCTACGACTTCACAATGTT-3′	5′-TTGATAGTCTCTCTGTCAGC-3′
CD86	5′-CTCTACGACTTCACAATGTT-3′	5′-TTGATAGTCTCTCTGTCAGC-3′
IL-1β	5′-AGTCAGGGTTCTTCCGTTAG-3′	5′-ACCTGTAAGGAGTGACACCA-3′
IL-6	5′-AGTTTTCCACCGTAAAGTGT-3′	5′-CGTCTCAAGGGGTTGACCAT-3′
IL-10	5′-GGATTTAGAGACTTGCTCTT-3′	5′-GTTTTAGCTTTTCATTTTGA-3′
STAT1	5′-TGCCGTGGAGCCCTACACGA-3′	5′-GCTCCATCGGTTCTGGTGCTTCC-3′

and cells were incubated for 20 min at 4°C in the dark and washed twice with ice-cold PBS. Fluorescence was measured with a FACScan (Becton Dickinson, Heidelberg, Germany).

Statistical analysis

Statistical significance was calculated by ANOVA using GraphPad Prism software (version 5.01). For the experiments with two variables (Fig. 1B–F), two-way ANOVA was used; the remaining data were analyzed by one-way ANOVA. A p value <0.05 was considered statistically significant.

Results

Role of Zn^{2+} in NO release by macrophages

In the mouse macrophage cell line RAW 264.7, the fluorescent probe FluoZin-3 detects an elevation of free intracellular Zn^{2+} in response to LPS (Fig. 1A). Accordingly, an impact of Zn^{2+} on the TLR4-induced release of NO is investigated. To this end, the concentration of nitrite, a degradation product of NO, is taken as a measure for production of the short-lived NO. Addition of the membrane-permeable Zn^{2+} chelator TPEN before stimulation of primary murine bone marrow–derived macrophages (BMMs) with LPS (Fig. 1B) and of RAW 264.7 cells with LPS or *E. coli* (Fig. 1C, 1D) leads to a concentration-dependent increase of nitrite in the cell culture supernatants. Incubation of RAW 264.7 cells with equimolar concentrations of Zn^{2+} in addition to TPEN abolishes the effect of the chelator (Fig. 1C), confirming that TPEN augments NO production by chelation of Zn^{2+}. In contrast, increasing the intracellular Zn^{2+} concentration by addition of Zn^{2+} together with the ionophore pyrithione is without effect (Fig. 1D).

To exclude a contribution of the other NO synthases, eNOS and nNOS, the selective iNOS inhibitors 1400W and SMT are used. Both inhibitors completely abrogate LPS-induced NO production, regardless of the presence of TPEN (Fig. 1E, Supplemental Fig. 1A). This confirms that the entire NO production in response to LPS is mediated exclusively by iNOS. Next, the effect of zinc deficiency was investigated independently from TPEN by cultivating RAW 264.7 cells for 3 d either in CHELEX-treated medium (zinc depleted) or CHELEX-treated medium reconstituted with 10 μM Zn^{2+} (zinc sufficient). The NO release of RAW 264.7 cells cultivated in zinc-depleted medium is markedly higher than in cells cultivated in zinc-sufficient medium. Furthermore, addition of Zn^{2+} and pyrithione simultaneous to LPS stimulation diminishes NO production in cells grown in zinc-depleted medium (Fig. 1F).

iNOS activity is mainly regulated on the transcriptional level. Accordingly, iNOS transcription in response to LPS stimulation of RAW 264.7 cells is elevated in the presence of TPEN (Fig. 2A). Notably, these conditions do not affect cellular viability (Supplemental Fig. 1B), and iNOS transcription is unaffected by TPEN alone (Supplemental Fig. 1C). Furthermore, iNOS protein expression after LPS stimulation is also increased by TPEN in a concentration-dependent manner (Fig. 2B). Altogether, the LPS-induced NO release is increased by Zn^{2+} chelation through elevated iNOS expression.

Impact of Zn^{2+} chelation on TLR4 signaling

TPEN has a differential impact on the mRNA expression of LPS-inducible genes. In contrast with iNOS, the LPS-induced transcription of IL-1β, IL-6, and IL-10 is significantly reduced by incubation of RAW 264.7 cells with the chelator (Fig. 3). On the other hand, transcription of type 1 IFNs is upregulated by Zn^{2+} chelation, in particular, IFN-β (Fig. 3). Rantes transcription is only reduced by 1.25 μM TPEN, the lowest applied TPEN concentration, and there is no effect of TPEN on MCP-1 and IP-10 (Fig. 3). The transcription of the cell-surface protein CD40 is slightly increased, but the effect is not statistically significant. CD80 and CD86 transcription is significantly elevated (Fig. 3). The gene transcription pattern suggests differential effects of Zn^{2+} chelation on MyD88 and TRIF-dependent TLR4 signaling, reducing MyD88 signaling whereas promoting the TRIF-dependent pathway. Activation of the two pathways is balanced through endocytosis of

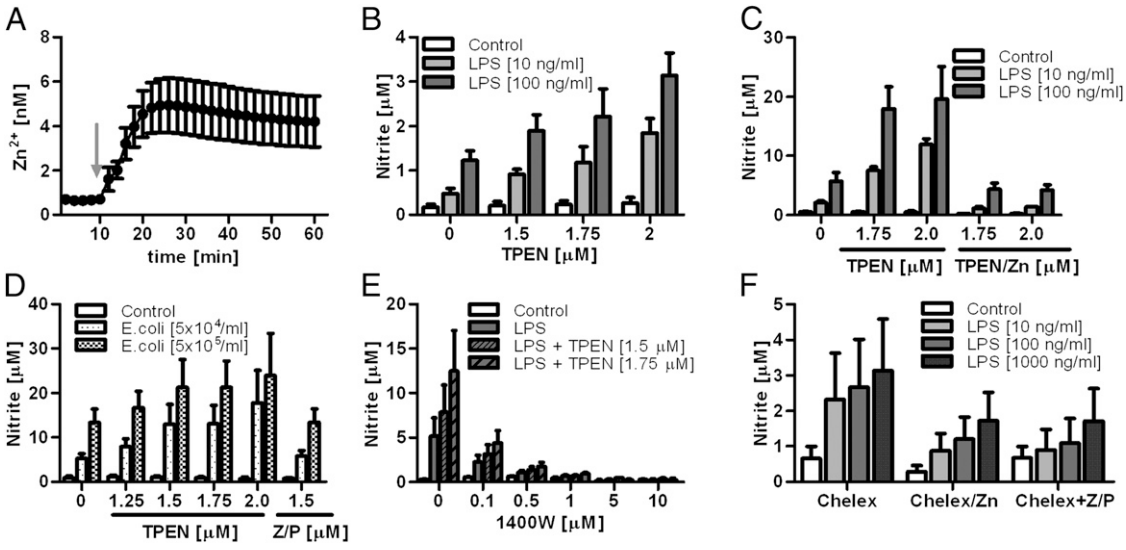

FIGURE 1. Impact of free intracellular Zn^{2+} on nitrite production. (**A**) RAW 264.7 cells were loaded with FluoZin-3. After 10 min measuring the baseline fluorescence, LPS (10 μg/ml) was added (arrow) and the fluorescence measured for additional 50 min. (**B**–**F**) Nitrite concentrations in the supernatants were determined with the Griess assay after 24-h incubation under the following conditions. (B) BMMs were incubated as indicated with TPEN (5 min before LPS) and LPS. (C) RAW 264.7 cells were preincubated for 5 min with different concentrations of TPEN or TPEN and Zn^{2+} (1:1 molar ratio) and stimulated with LPS. (D) RAW 264.7 cells were preincubated for 5 min with TPEN or Zn^{2+}/pyrithione (Z/P, both 1.5 μM) and stimulated with heat-killed *E. coli*. (E) RAW 264.7 cells were preincubated with TPEN for 5 min and stimulated with LPS (100 ng/ml) in the presence of the iNOS inhibitor 1400W. (F) RAW 264.7 cells were grown for 3 d either in zinc-depleted medium (CHELEX) alone or reconstituted with 10 μM Zn^{2+} (CHELEX/Zn). Subsequently, cells were stimulated as indicated with LPS. Zn^{2+}/pyrithione (both 1.5 μM) were added to cells grown in zinc-depleted medium (CHELEX+Z/P) simultaneously to LPS. All data are shown as means ± SEM of at least $n = 3$ independent experiments. There was a statistically significant impact on nitrite production by TPEN (B–D; $p < 0.001$) and by CHELEX (F; $p = 0.0011$; two-way ANOVA).

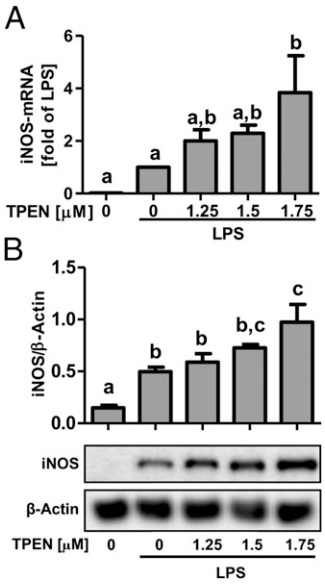

FIGURE 2. Effect of TPEN on iNOS induction. (**A**) iNOS mRNA in RAW 264.7 cells after 5-min preincubation with TPEN and 4-h stimulation with LPS (100 ng/ml). Results are normalized to LPS-treated control and represent means + SEM of $n = 7$ independent experiments. (**B**) iNOS protein in RAW 264.7 cells was measured by Western blotting after preincubation with TPEN and 10-h stimulation with 100 ng/ml LPS. Results show means + SEM of densitometric quantifications (*upper panel*) and one representative (*lower panel*) from $n = 8$ independent experiments. (A and B) Data were analyzed by repeated-measures ANOVA and Tukey post hoc test. Significantly different means do not share the same letters.

the TLR4R complex (10). However, the LPS-induced endocytosis of TLR4 is not affected by TPEN (Fig. 4A). TRAF3-ubiquitination is another mode of balancing MyD88 and TRIF-dependent signaling. TRAF3 is ubiquitinated on Lys^{48} for MyD88 signaling (with subsequent degradation), whereas it is ubiquitinated on Lys^{63} for TRIF signaling (23). No TRAF3 degradation is induced in BMMs treated from 15 min to 3 h with LPS, independently of TPEN preincubation (Fig. 4B).

A time-dependent comparison between the activation of the transcription factors NF-κB and IRF3 was made in whole cells and nuclear extracts (Fig. 4C, 4D). The MyD88-dependent early nuclear translocation of NF-κB 30 min and 1 h after LPS stimulation is reduced in the presence of TPEN. In contrast, the TRIF-dependent delayed NF-κB activation after 2 and 3 h is not diminished by TPEN. IRF3 phosphorylation is detected in the whole-cell lysate starting at 1 h (Fig. 4D). After 2 and 3 h, phospho-IRF3 is found in the nucleus and in whole cells, but only nuclear phospho-IRF3 is increased by TPEN (Fig. 4C, 4D). Hence, Zn^{2+} chelation upregulates TRIF signaling upstream of the transcription factor IRF3 and leads to increased nuclear accumulation of phospho-IRF3.

To further evaluate the time dependence of Zn^{2+} chelation for the enhancement of NO release, we added TPEN at different time points relative to LPS, ranging from 5 min prior (as in the previous experiments) to 8 h after addition of the TLR ligand. The addition of TPEN 5 min before LPS stimulation doubles NO release in comparison with LPS alone, but the effect is even more pronounced at 30 min to 1 h after LPS stimulation (Fig. 4E). Starting 2 h after LPS stimulation, the effect of TPEN addition decreases slightly, but up to 8 h after LPS stimulation still increases NO release ~2.5 times compared with LPS alone. By this time, the LPS-induced zinc signal has already returned to baseline levels (Fig. 4F). Hence, the effect of Zn^{2+} chelation is most effective at the time when the TRIF pathway is activated, and basal Zn^{2+} levels, not the initial zinc signal, alter NO release.

Involvement of IFN-β in the impact of Zn^{2+} chelation on iNOS

The main function of IRF3 in monocytes is the induction of IFN-β. Because IFN-β transcription is elevated by Zn^{2+} chelation, the

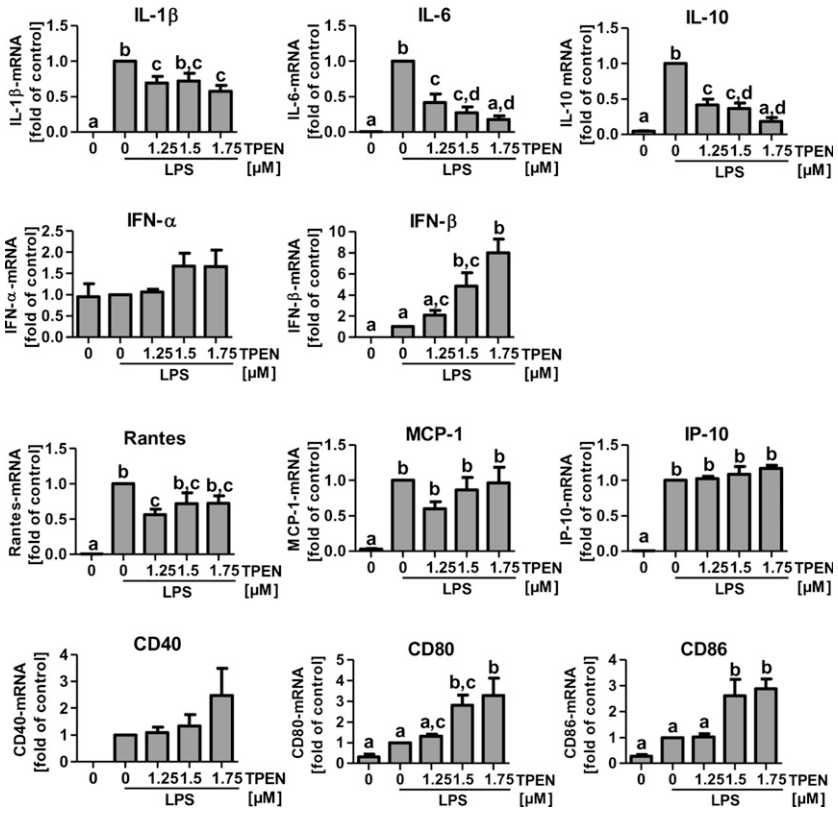

FIGURE 3. Effect of TPEN on the transcription of LPS-induced genes. The effects of 5-min preincubation with TPEN on mRNA expression after stimulation of RAW 264.7 cells with LPS (100 ng/ml, 4 h) was analyzed for IL-1β, IL-6, IL-10, IFN-α, IFN-β, Rantes, MCP-1, IP-10, CD40, CD80, and CD86. Results are normalized to the LPS-treated control and represent means + SEM of $n = 5$ independent experiments. Data were analyzed by repeated-measures ANOVA and Tukey post hoc test. Significantly different means do not share the same letters.

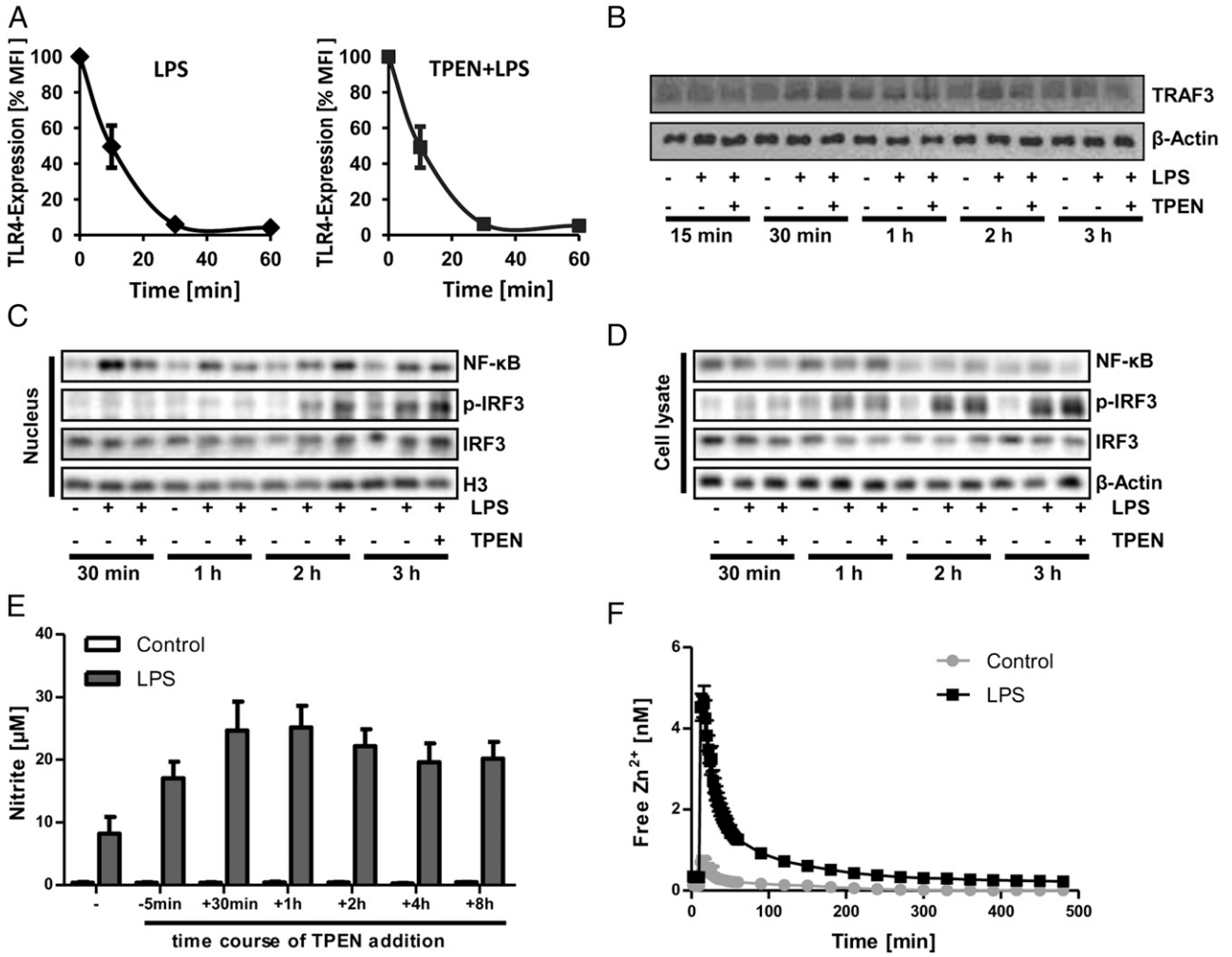

FIGURE 4. Impact of Zn^{2+} chelation on TLR4 signaling. (**A**) Surface expression of TLR4 after stimulation with LPS (100 ng/ml) alone or in the presence of TPEN (1.75 μM, 5 min before LPS) was measured by flow cytometry. (**B**) Western blot of TRAF3 protein levels in BMMs after stimulation with LPS (100 ng/ml) alone or in the presence of TPEN (1.75 μM, 5 min before LPS). (**C** and **D**) RAW 264.7 cells were stimulated for the indicated times with LPS (100 ng/ml) and TPEN (5 min before LPS). Western blots for NF-κB, phosphorylated (Ser^{396}) and total IRF3 were performed with nuclear extracts (C) and whole cells (D), using histone H3 and β-actin as respective housekeeping genes. (**E**) RAW 264.7 cells were incubated with LPS (100 ng/ml), and TPEN (1.75 μM) was added at different time points relative to LPS as indicated. A Griess assay was performed with the supernatant 24 h after addition of LPS. (**F**) Intracellular Zn^{2+} was measured as described for Fig. 1A. After the first hour, measurements were made in 30-min intervals. Results are shown as means ± SEM of $n = 3$ independent experiments (A, E, F) or one representative experiment of $n = 3$ (B–D).

impact of supplementation with additional IFN-β on NO release was examined. Stimulation with a high amount of IFN-β (2000 U/ml) alone does not induce the release of NO but augments LPS-induced NO release in a manner similar to TPEN. Notably, TPEN does not cause a further increase of NO production (Fig. 5A, Supplemental Fig. 2A) and iNOS protein levels (Fig. 5B; Supplemental Fig. 2B) in the presence of IFN-β. Purified rat IgG1 Abs against murine IFN-β cause a concentration-dependent reduction of LPS-induced NO release by RAW 264.7 cells treated with LPS and LPS+TPEN (Fig. 5C). Together, these results imply that Zn^{2+} chelation augments the NO release through increased IFN-β levels.

IFN-β activates a JAK-STAT pathway; hence the impact of Zn^{2+} chelation on STAT1 phosphorylation was investigated. RAW 264.7 cells were preincubated with TPEN and stimulated with IFN-β. Western blot analysis of STAT1 phosphorylation shows no effect of TPEN on Tyr^{701} and Ser^{727} phosphorylation. However, there is a slight decrease in total STAT1 protein in TPEN-preincubated and IFN-β–stimulated samples (Fig. 5D, Supplemental Fig. 2C). Consequently, transcription of STAT1 mRNA after preincubation with TPEN and stimulation with LPS or IFN-β was measured. Stimulation increases STAT1 expression, which is abrogated by preincubation with TPEN (Fig. 5E, 5F, Supplemental Fig. 2D). Together, Zn^{2+} chelation has no effect on IFN-β–induced STAT1 phosphorylation while reducing its transcription.

Role of Zn^{2+} in NO release in response to other receptors

To elucidate whether zinc signals are relevant for signaling by other TLRs in addition to TLR4, we tested a panel of different ligands. Stimulation of RAW 264.7 cells with pam3CSK4 (TLR1/2 ligand), heat-killed *Listeria monocytogenes* (TLR2 ligand), flagellin (TLR5 ligand), FSL-1 (TLR6/2 ligand), imiquimod and ssRNA40 (TLR7 ligands), and ODN1826 (TLR9 ligand) induces zinc signals (Fig. 6). The only examined TLR ligand unable to induce a zinc signal is poly(I:C) (TLR3 ligand; Fig. 6). Comparable observations were made using human primary monocytes (Supplemental Fig. 3). The inability of poly(I:C) to induce a zinc signal was confirmed in RAW 264.7 with the fluorescent probe ZinPyr1 (Supplemental Fig. 4A), and biological activity of the poly(I:C) in RAW 264.7 cells was confirmed by measuring TNF-α secretion (Supplemental Fig. 4B).

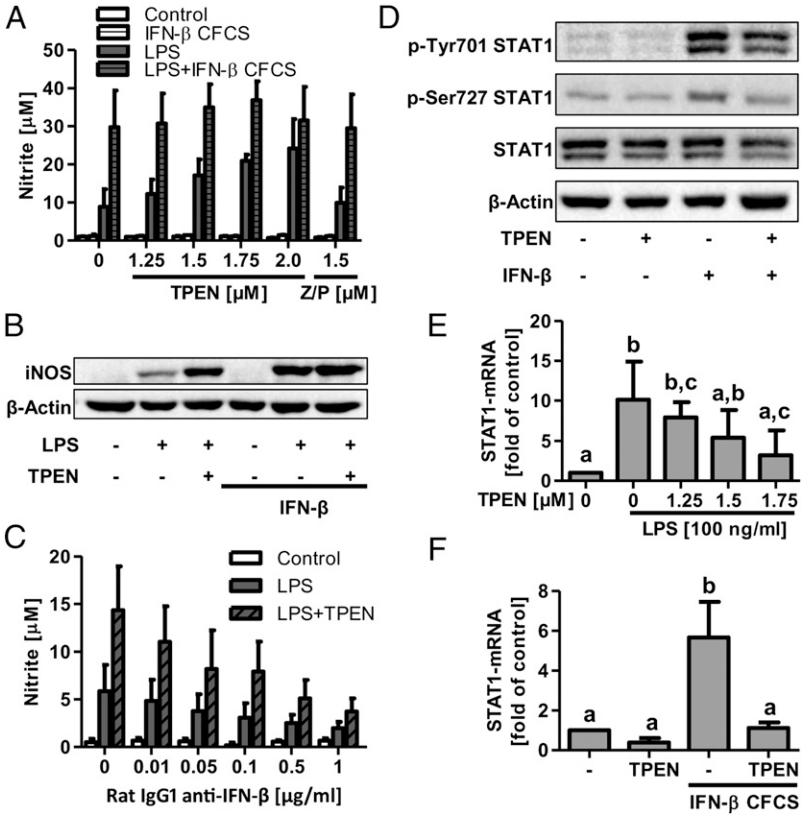

FIGURE 5. Role of IFN-β in iNOS induction. (**A**) Nitrite was quantified in supernatants from RAW 264.7 cells preincubated with different concentrations of TPEN or Zn^{2+}/pyrithione (Z/P, both 1.5 μM) and stimulated for 24 h with LPS (100 ng/ml) and IFN-β (2000 U/ml; 293T cell-free culture supernatant [CFCS]) or unconditioned control medium. (**B**) RAW 264.7 cells were incubated for 10 h as described for (A), and iNOS expression was determined by Western blotting. (**C**) Nitrite was quantified in supernatants from RAW 264.7 cells preincubated with TPEN (1.75 μM) and stimulated for 24 h with LPS (100 ng/ml) in the presence of purified rat IgG1 Abs against murine IFN-β. (**D**) RAW 264.7 cells were incubated for 3 h with TPEN (1.75 μM) and additionally for 30 min with IFN-β (2000 U/ml; 293T CFCS) or unconditioned control medium. Phosphorylation of STAT1 at Tyr^{701} and Ser^{727} was determined by Western blotting. (**E** and **F**) STAT1 mRNA was determined in RAW264.7 cells. (E) Five-minute preincubation with TPEN was followed by 4-h stimulation with LPS (100 ng/ml). (F) Five-minute preincubation with TPEN (1.75 μM) was followed by 4-h stimulation with IFN-β (2000 U/ml; 293T CFCS) or unconditioned control medium. (A, C, E, and F) Results are shown as means + SEM of $n = 3$ or (B, D) one representative of $n = 3$ independent experiments. (E, and F) Data were analyzed by repeated-measures ANOVA and Tukey post hoc test. Significantly different means do not share the same letters.

Further investigations determined the effect of Zn^{2+} chelation on NO release induced by another TLR that triggered a zinc signal, TLR7, and by TLR3, which is inactive with respect to zinc signaling. Comparable with LPS, the TLR7 ligand imiquimod induces the release of NO, which can be further elevated by TPEN (Fig. 7A). iNOS protein expression is also increased by incubation of imiquimod-stimulated RAW 264.7 cells with TPEN (Fig. 7B). Similar to TLR4, Zn^{2+} chelation affected the transcription of several genes. Whereas the mRNA levels of IL-1β and IL-6 are unaltered by TPEN, there is a significant decrease of IL-10 mRNA (Fig. 7C). Comparable with the observations with TLR4, the levels of IFN-α, IFN-β, CD40, CD80, and CD86 mRNA are increased, although the effect is only statistically significant for IFN-β, CD80, and CD86 (Fig. 7C). The effect of TPEN on TLR3-induced NO release and IFN-β mRNA transcription was also examined. NO release in response to poly(I:C) increases in a concentration-dependent manner in TPEN-treated samples (Fig. 7D). In addition, IFN-β transcription is elevated after preincubation with TPEN and stimulation with poly(I:C) (Fig. 7E). Similar to the effect on TLR4 signaling, increasing the intracellular free Zn^{2+} concen-

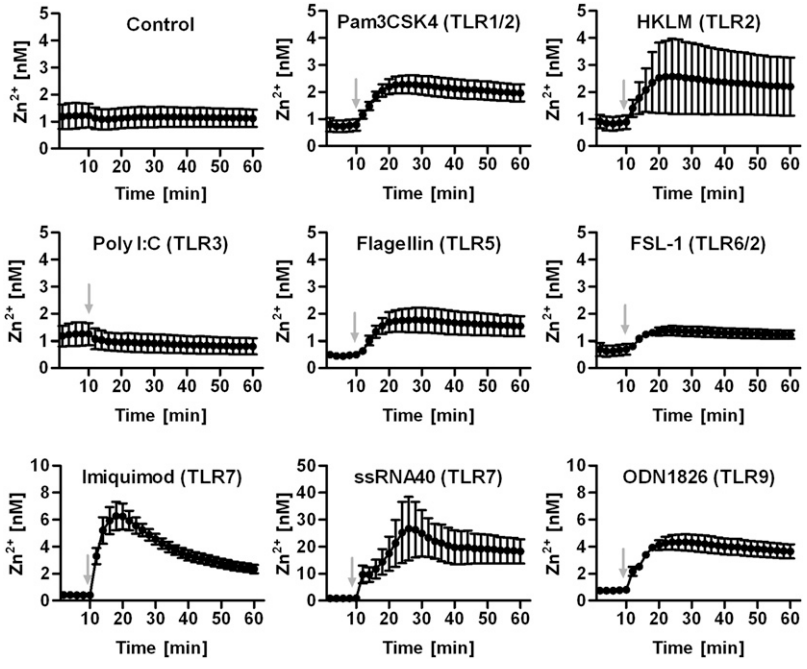

FIGURE 6. TLR-induced zinc signals in RAW 264.7 cells. Intracellular Zn^{2+} was measured as described for Fig. 1A. RAW 264.7 cells were stimulated with Pam3CSK4 (1 μg/ml), heat-killed *L. monocytogenes* (HKLM, 10^7/ml), poly(I:C) (10 μg/ml), *Salmonella typhimurium* flagellin (1 μg/ml), FSL-1 (1 μg/ml), imiquimod (10 μg/ml), ssRNA40 (1 μg/ml), or ODN1826 (10 μg/ml). Data are shown as means ± SEM of at least $n = 3$ independent experiments.

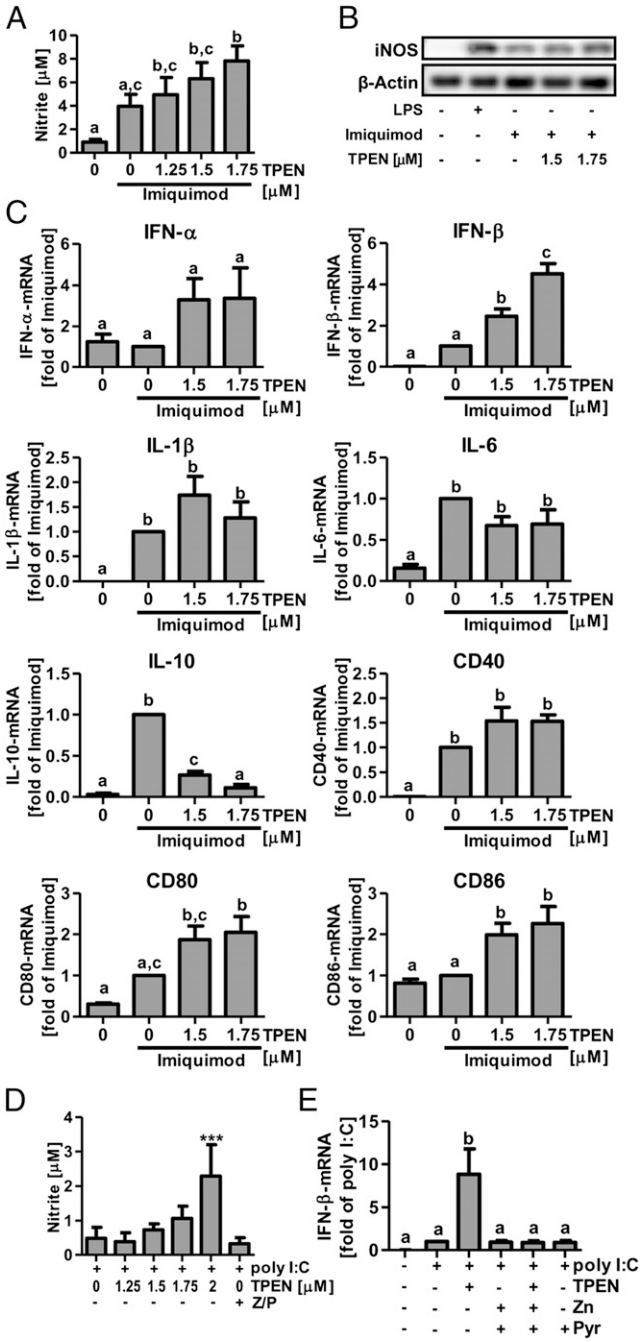

FIGURE 7. Impact of Zn^{2+} chelation on TLR3- and TLR7-induced iNOS induction. (**A**) RAW 264.7 cells were preincubated with TPEN (5 min) before addition of imiquimod (1 μg/ml, 24 h), followed by nitrite determination with a Griess assay. (**B**) iNOS protein expression in RAW 264.7 cells was determined by Western blotting after 5-min preincubation with TPEN and stimulation for 24 h with imiquimod (1 μg/ml) or LPS (100 ng/ml). (**C**) mRNA levels of IL-1β, IL-6, IL-10, IFN-α, IFN-β, CD40, CD80, and CD86 in RAW 264.7 cells treated with TPEN (5 min before imiquimod) and imiquimod (1 μg/ml, 4 h). Results are normalized to the imiquimod-treated controls. (**D**) RAW 264.7 cells were stimulated with poly(I:C) (1 μg/ml) 5 min after addition of TPEN or Zn^{2+}/pyrithione (Z/P, both 1.5 μM). Statistically significant differences to the untreated control are indicated (repeated-measures ANOVA with Dunnett post hoc test; $***p < 0.001$). (**E**) IFN-β mRNA levels were determined in RAW 264.7 cells after 4-h stimulation with poly(I:C) (1 μg/ml) after addition of TPEN (1.75 μM), Zn^{2+} (Zn, 1.75 μM), and pyrithione (Pyr, 1.75 μM) as indicated. Results are normalized to the untreated control. Results are shown as means + SEM (A, C–E) or one representative blot (B) of at least $n = 3$ independent experiments. Data in (A, C, E) were analyzed by repeated-measures ANOVA and Tukey post hoc test. Significantly different means do not share the same letters.

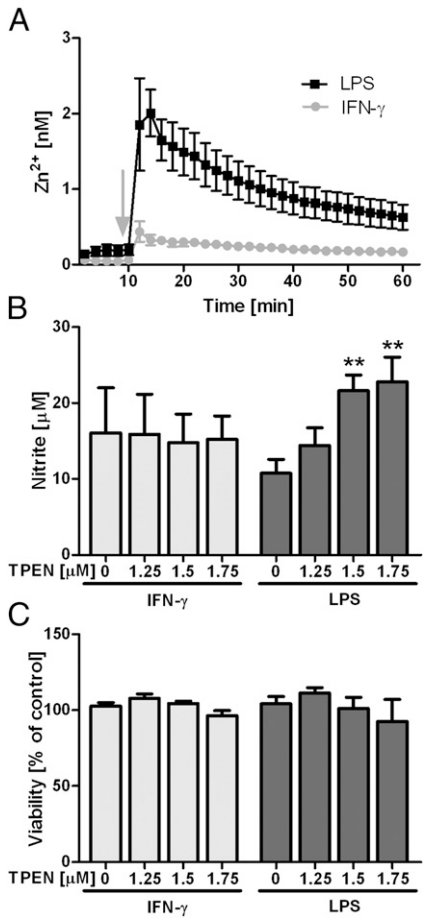

FIGURE 8. Role of Zn^{2+} in IFN-γ–induced NO release. (**A**) Intracellular Zn^{2+} was measured as described for Fig. 1A. RAW 264.7 cells were stimulated with LPS (1 μg/ml) or IFN-γ (500 U/ml). (**B**) Supernatant nitrite concentrations of RAW264.7 cells were determined with the Griess assay after 24-h incubation with TPEN (5 min before LPS/IFN), IFN-γ (500 U/ml), or LPS (100 ng/ml). Statistically significant differences to the respective controls are indicated (repeated-measures ANOVA with Dunnett's post hoc test; $**p < 0.01$). (**C**) Survival of RAW 264.7 cells incubated as indicated with TPEN, IFN-γ (500 U/ml), or LPS (100 ng/ml) was determined by neutral red assay. All data are shown as means from at least $n = 3$ independent experiments ± SEM.

tration by addition of Zn^{2+} and pyrithione does not alter TLR3-mediated NO release or IFN-β transcription (Fig. 7D, 7E).

IFN-γ induces iNOS expression independently from IFN-β (24). In contrast with LPS, IFN-γ does not trigger a zinc signal (Fig. 8A) and IFN-γ–mediated NO production is not augmented by TPEN (Fig. 8B). Notably, the absence of TPEN-induced elevation of iNOS activity is not due to toxicity of the chelator in combination with IFN-γ (Fig. 8C). Consequently, regulation by free Zn^{2+} is not a general feature of iNOS expression but is specific for the TRIF/IRF/IFN-β pathway.

Discussion

Binding of LPS to TLR4 leads to recruitment of the adaptor proteins TIRAP and MyD88, resulting in the early activation of NF-κB, triggering mRNA expression of inflammatory cytokines (25). Subsequently, the receptor complex is internalized and binds TRAM and TRIF, inducing the delayed activation of NF-κB and phosphorylation of IRF3. Phosphorylated IRF3 translocates into the nucleus and induces the transcription of IFN-β (25). In turn, IFN-β production is essential for LPS-induced iNOS expression (17), because IFN-β activates the type I IFNR and the JAK-STAT

pathway in an autocrine and paracrine fashion (16). Together, NF-κB and STAT1 induce iNOS transcription (15).

Activation of TLR4 also triggers a zinc signal. It supports MAPK signaling through inhibition of dephosphorylation, and is required for the phosphorylation of IKKα/β and for NF-κB–dependent production of inflammatory cytokines (7). This involvement of a zinc signal in MyD88 signaling is confirmed by this study. After TLR4 or TLR7 stimulation, the transcription of NF-κB–dependent genes such as IL-1β, IL-6, and IL-10 decreased, at least to some extent, when the zinc signal was chelated by TPEN. In addition, Zn^{2+} chelation reduced the MyD88-dependent nuclear translocation of NF-κB. Nevertheless, free intracellular Zn^{2+} is not an unspecific activator of all aspects of TLR signaling. The transcription of TRIF-dependent genes, such as IFN-β and the IFN-β–induced genes CD80 and CD86, is enhanced by Zn^{2+} chelation. Moreover, the Zn^{2+} chelator TPEN increases LPS-induced NO release through upregulation of iNOS expression. Simultaneously, there is no distinct effect of Zn^{2+} chelation on the TRIF-dependent genes Rantes, IP-10, and MCP-1. All three genes are thought to be mainly induced by TRIF signaling (26), but, possibly, other signaling pathways such as PI3K, NF-κB, and the MAPK ERK are also involved in TLR-dependent induction of Rantes, MCP-1, and IP-10 (27, 28), explaining the differential outcome.

Signaling via several homodimers and heterodimers of TLR1-9 induces zinc signals, with TLR3 being the only exception. Notably, TLR3 is also the only TLR that does not activate the MyD88 pathway (29) but is capable of inducing IFN and iNOS expression via TRIF-dependent activation of NF-κB and IRF3 (30). Hence, not only does the zinc signal selectively support MyD88-dependent signaling, it only occurs in response to stimulation of TLRs triggering that particular pathway. Nevertheless, LPS-induced zinc signals occur in BMMs isolated from MyD88 knockout mice; therefore, the adaptor molecule itself is not required for the induction of zinc signals (7).

To identify the aspect(s) of TRIF signaling that are negatively regulated by Zn^{2+}, we investigated several details of the pathway. Endocytosis of TLR4 was not altered by Zn^{2+} chelation, pointing toward an impact of Zn^{2+} that is located downstream of receptor internalization. Also, TRAF3 degradation was not involved. In contrast, an increase of nuclear, but not total cellular phospho-IRF3, was measured in response to Zn^{2+} chelation. This suggests that Zn^{2+} affects nuclear phosphorylation of IRF3, or nuclear translocation or retention of phospho-IRF3. Furthermore, TLR7-induced IFN-β and iNOS transcription also increases by Zn^{2+} chelation, but TLR7 signals via MyD88 and IRF7. IRF3 activation depends on phosphorylation by TBK1 and IKKε (31). The kinases are activated by the recruitment of TRAF3 to TRIF (32) and Lys^{63} ubiquitination of TRAF3 (23). IRF7, in contrast, is phosphorylated by the kinases IL-1R–associated kinase 1 and IKK-α (33). Unphosphorylated IRF3 shuttles between cytoplasm and nucleus with nuclear export being the predominant effect (34, 35). Transport proteins for IRF3 import are a subset of importin-α receptors, namely, Qip1 and KPNA3, which associate with importin-β receptors and the small GTPase Ran. Nuclear export is mediated by chromosome region maintenance/exportin 1 (34). Phosphorylated IRF3 and IRF7 bind to the histone acetylases CREB-binding protein and p300 (35, 36), and are localized in the nucleus through retention by CREB-binding protein/p300 (35). Therefore, activation and nuclear translocation of IRF3, as well as IRF7, offer many possibilities for regulation by Zn^{2+}, which should be elucidated in more detail in future investigations.

Enhancement of iNOS induction by Zn^{2+} chelation also depends on the IRF3-dependent increase in IFN-β production. NO release was almost completely abrogated by an IFN-β–specific Ab, and more importantly, TPEN was ineffective in the presence of excess IFN-β. Further downstream, a potential influence of Zn^{2+} chelation on the IFN-β–dependent activation of the STAT pathway was examined. Treatment of cells with TPEN had no effect on IFN-β–mediated STAT1 phosphorylation. A comparable result has been observed for STAT5 phosphorylation in response to stimulation of the T cell line CTLL-2 with IL-2 (37), indicating that zinc signals might not be involved in JAK/STAT phosphorylation signaling by cytokine receptors in general. In contrast, TPEN reduced STAT1 transcription in response to stimulation with LPS or IFN-β. This finding will have no impact on the signaling events described in this article because the reported half-life for STAT1 is 16 h (38). It could, however, affect long-term signaling via the IFN-βR, representing a possible feedback mechanism to limit iNOS induction in response to prolonged exposure to LPS. This effect also could influence the subsequent activation of other signaling pathways involving STAT1 phosphorylation and signals depending on the level of unphosphorylated STAT1 protein for transcriptional activity (39).

Zn^{2+} frequently mediates its effects on signal transduction by inhibiting protein tyrosine phosphatases (PTPs) (40). PTPs known to be involved in TRIF signaling are SHP-2, SHIP1, and PTP1B (41–43). Nevertheless, all three PTPs are negative regulators of TRIF signaling, and activating them by reducing free Zn^{2+} could not explain augmentation of the TRIF pathway (41–43). Moreover, the reduction of basal intracellular Zn^{2+} concentrations modifies TRIF signaling, whereas most PTP inhibition constants measured so far are higher than basal intracellular Zn^{2+} level; for example, PTP1B is inhibited by Zn^{2+} with an IC_{50} of 17 nM (40), a concentration that is well above the basal intracellular Zn^{2+} measured in monocytes (6). Yet, there is significant divergence in the inhibition constants of different PTP for Zn^{2+}. For the RPTPβ, an inhibition constant of 21 pM was recently shown, indicating

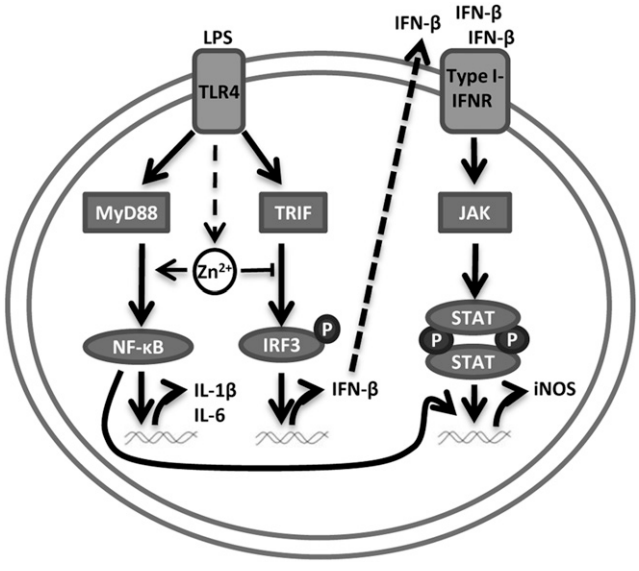

FIGURE 9. Scheme of the role of Zn^{2+} in TLR4 signaling. TLR4 signals via two main pathways involving the adaptor proteins MyD88 or TRIF. MyD88-dependent signaling induces early activation of the transcription factor NF-κB, leading to the production of inflammatory cytokines, such as IL-1β and IL-6. TRIF-dependent signaling causes a delayed activation of NF-κB (not shown for reasons of clarity) and IRF3, resulting in the production of IFN-β. In turn, IFN-β activates the type I IFNR and its corresponding JAK-STAT pathway in an autocrine and paracrine fashion, leading to the production of iNOS. Free intracellular Zn^{2+} has a differential impact on both pathways, augmenting MyD88-dependent signaling whereas inhibiting TRIF-mediated activation of IRF3.

that under normal conditions, RPTPβ could exist predominantly in its Zn^{2+}-bound inactive state, being activated by a reduction of basal Zn^{2+} levels (44). Consequently, there may be one or more PTPs positively regulating TRIF signaling, which are controlled by intracellular free Zn^{2+} in a similar manner. It was suggested that Zn^{2+} inhibits PTPs by binding to a catalytically active thiol in the active site (45). Other enzymes, such as deubiquitinases, also have thiols in their catalytic center with a comparably low pKa, and hence similar chemical reactivity, which is illustrated by the fact that both classes of enzymes can be inactivated reversibly by thiol oxidation (46). It is conceivable that these enzymes also have a similar reactivity toward Zn^{2+}, making them potential molecular targets for an effect of Zn^{2+} in addition to PTPs.

Dendritic cell maturation in response to LPS and monocytic differentiation of myeloid precursors stimulated by calcitriol both depend on alterations of cellular zinc homeostasis, ultimately leading to reduced free Zn^{2+} (20, 47). This shows that Zn^{2+} exerts regulatory functions not only through short-term spikes, but also via modulation of basal Zn^{2+} levels. Both effects are combined in TLR4 signaling, balancing MyD88 and TRIF signaling (Fig. 9). After the initial increase in free Zn^{2+}, facilitating MyD88 signaling, the concentration returns to basal values within a few hours, but these are still sufficiently high to limit TRIF signaling.

The reaction of macrophages toward TLR stimulation is multifaceted. An inflammatory immune response is triggered through MyD88-dependent production of cytokines, such as IL-1β and IL-6. In addition, TLRs induce an antiviral immune response through TRIF-mediated release of IFN-β (48). TLR-induced NO release has various effects. NO is involved in antimicrobial, antiviral, and antitumor immune defense, but can also damage host tissue and suppress beneficial as well as harmful immune responses (49). This is of particular importance for the adequate activation of innate immunity. On the one hand, TLRs are necessary for the induction of protective immunity against infection; on the other hand, an inappropriate TLR response is associated with acute and chronic inflammation and systemic autoimmune diseases (48). This study identifies free Zn^{2+} ions as a signal differentially affecting all of these functions at multiple levels, hereby fine-tuning TLR signaling.

Acknowledgments

We thank Prof. Dr. R. Zawatzky (Deutsches Krebsforschungszentrum Heidelberg, Heidelberg, Germany) for the 7FD3 hybridoma cell line and the 3T3 and 293T cell lines transfected to produce IFN-β. We also thank Silke Hebel and Gabriela Engelhardt for technical assistance.

Disclosures

The authors have no financial conflicts of interest.

References

1. Prasad, A. S., F. W. Beck, B. Bao, J. T. Fitzgerald, D. C. Snell, J. D. Steinberg, and L. J. Cardozo. 2007. Zinc supplementation decreases incidence of infections in the elderly: effect of zinc on generation of cytokines and oxidative stress. *Am. J. Clin. Nutr.* 85: 837–844.
2. Haase, H., and L. Rink. 2009. The immune system and the impact of zinc during aging. *Immun. Ageing* 6: 9.
3. Haase, H., and L. Rink. 2009. Functional significance of zinc-related signaling pathways in immune cells. *Annu. Rev. Nutr.* 29: 133–152.
4. Cousins, R. J., J. P. Liuzzi, and L. A. Lichten. 2006. Mammalian zinc transport, trafficking, and signals. *J. Biol. Chem.* 281: 24085–24089.
5. Kojima, C., A. Kawakami, T. Takei, K. Nitta, and M. Yoshida. 2007. Angiotensin-converting enzyme inhibitor attenuates monocyte adhesion to vascular endothelium through modulation of intracellular zinc. *J. Pharmacol. Exp. Ther.* 323: 855–860.
6. Haase, H., S. Hebel, G. Engelhardt, and L. Rink. 2006. Flow cytometric measurement of labile zinc in peripheral blood mononuclear cells. *Anal. Biochem.* 352: 222–230.
7. Haase, H., J. L. Ober-Blöbaum, G. Engelhardt, S. Hebel, A. Heit, H. Heine, and L. Rink. 2008. Zinc signals are essential for lipopolysaccharide-induced signal transduction in monocytes. *J. Immunol.* 181: 6491–6502.
8. Medzhitov, R. 2009. Approaching the asymptote: 20 years later. *Immunity* 30: 766–775.
9. Botos, I., D. M. Segal, and D. R. Davies. 2011. The structural biology of Toll-like receptors. *Structure* 19: 447–459.
10. Kagan, J. C., T. Su, T. Horng, A. Chow, S. Akira, and R. Medzhitov. 2008. TRAM couples endocytosis of Toll-like receptor 4 to the induction of interferon-beta. *Nat. Immunol.* 9: 361–368.
11. Fitzgerald, K. A., D. C. Rowe, B. J. Barnes, D. R. Caffrey, A. Visintin, E. Latz, B. Monks, P. M. Pitha, and D. T. Golenbock. 2003. LPS-TLR4 signaling to IRF-3/7 and NF-kappaB involves the toll adapters TRAM and TRIF. *J. Exp. Med.* 198: 1043–1055.
12. Monroe, K. M., S. M. McWhirter, and R. E. Vance. 2010. Induction of type I interferons by bacteria. *Cell. Microbiol.* 12: 881–890.
13. Hoebe, K., E. M. Janssen, S. O. Kim, L. Alexopoulou, R. A. Flavell, J. Han, and B. Beutler. 2003. Upregulation of costimulatory molecules induced by lipopolysaccharide and double-stranded RNA occurs by Trif-dependent and Trif-independent pathways. *Nat. Immunol.* 4: 1223–1229.
14. Lien, E., and D. T. Golenbock. 2003. Adjuvants and their signaling pathways: beyond TLRs. *Nat. Immunol.* 4: 1162–1164.
15. Farlik, M., B. Reutterer, C. Schindler, F. Greten, C. Vogl, M. Müller, and T. Decker. 2010. Nonconventional initiation complex assembly by STAT and NF-kappaB transcription factors regulates nitric oxide synthase expression. *Immunity* 33: 25–34.
16. Gao, J. J., M. B. Filla, M. J. Fultz, S. N. Vogel, S. W. Russell, and W. J. Murphy. 1998. Autocrine/paracrine IFN-alphabeta mediates the lipopolysaccharide-induced activation of transcription factor Stat1alpha in mouse macrophages: pivotal role of Stat1alpha in induction of the inducible nitric oxide synthase gene. *J. Immunol.* 161: 4803–4810.
17. Jacobs, A. T., and L. J. Ignarro. 2003. Cell density-enhanced expression of inducible nitric oxide synthase in murine macrophages mediated by interferon-beta. *Nitric Oxide* 8: 222–230.
18. Kröncke, K. D., K. Fehsel, C. Suschek, and V. Kolb-Bachofen. 2001. Inducible nitric oxide synthase-derived nitric oxide in gene regulation, cell death and cell survival. *Int. Immunopharmacol.* 1: 1407–1420.
19. Hill, B. G., B. P. Dranka, S. M. Bailey, J. R. Lancaster, Jr., and V. M. Darley-Usmar. 2010. What part of NO don't you understand? Some answers to the cardinal questions in nitric oxide biology. *J. Biol. Chem.* 285: 19699–19704.
20. Dubben, S., A. Hönscheid, K. Winkler, L. Rink, and H. Haase. 2010. Cellular zinc homeostasis is a regulator in monocyte differentiation of HL-60 cells by 1 alpha,25-dihydroxyvitamin D3. *J. Leukoc. Biol.* 87: 833–844.
21. Zawatzky, R., H. Wurmbaeck, W. Falk, and A. Homfeld. 1991. Endogenous interferon specifically regulates Newcastle disease virus-induced cytokine gene expression in mouse macrophages. *J. Virol.* 65: 4839–4846.
22. Griess, P. 1879. Bemerkungen zu der Abhandlung der HH. Weselsky und Benedikt ueber einige Azoverbindungen. *Berichte d. d. chem. Gesellschaft.* 12: 426–428.
23. Tseng, P. H., A. Matsuzawa, W. Zhang, T. Mino, D. A. Vignali, and M. Karin. 2010. Different modes of ubiquitination of the adaptor TRAF3 selectively activate the expression of type I interferons and proinflammatory cytokines. *Nat. Immunol.* 11: 70–75.
24. Schroder, K., P. J. Hertzog, T. Ravasi, and D. A. Hume. 2004. Interferon-gamma: an overview of signals, mechanisms and functions. *J. Leukoc. Biol.* 75: 163–189.
25. Ostuni, R., I. Zanoni, and F. Granucci. 2010. Deciphering the complexity of Toll-like receptor signaling. *Cell. Mol. Life Sci.* 67: 4109–4134.
26. Yamamoto, M., S. Sato, H. Hemmi, K. Hoshino, T. Kaisho, H. Sanjo, O. Takeuchi, M. Sugiyama, M. Okabe, K. Takeda, and S. Akira. 2003. Role of adaptor TRIF in the MyD88-independent toll-like receptor signaling pathway. *Science* 301: 640–643.
27. Mitchell, D., and C. Olive. 2010. Regulation of Toll-like receptor-induced chemokine production in murine dendritic cells by mitogen-activated protein kinases. *Mol. Immunol.* 47: 2065–2073.
28. Orita, T., K. Kimura, T. Nishida, and K. H. Sonoda. 2013. Cytokine and chemokine secretion induced by poly(I:C) through NF-κB and phosphoinositide 3-kinase signaling pathways in human corneal fibroblasts. *Curr. Eye Res.* 38: 53–59.
29. Kawai, T., and S. Akira. 2007. TLR signaling. *Semin. Immunol.* 19: 24–32.
30. Hiscott, J., T. L. Nguyen, M. Arguello, P. Nakhaei, and S. Paz. 2006. Manipulation of the nuclear factor-kappaB pathway and the innate immune response by viruses. *Oncogene* 25: 6844–6867.
31. Fitzgerald, K. A., S. M. McWhirter, K. L. Faia, D. C. Rowe, E. Latz, D. T. Golenbock, A. J. Coyle, S. M. Liao, and T. Maniatis. 2003. IKKepsilon and TBK1 are essential components of the IRF3 signaling pathway. *Nat. Immunol.* 4: 491–496.
32. Oganesyan, G., S. K. Saha, B. Guo, J. Q. He, A. Shahangian, B. Zarnegar, A. Perry, and G. Cheng. 2006. Critical role of TRAF3 in the Toll-like receptor-dependent and -independent antiviral response. *Nature* 439: 208–211.
33. Blasius, A. L., and B. Beutler. 2010. Intracellular toll-like receptors. *Immunity* 32: 305–315.
34. Reich, N. C. 2002. Nuclear/cytoplasmic localization of IRFs in response to viral infection or interferon stimulation. *J. Interferon Cytokine Res.* 22: 103–109.
35. Kumar, K. P., K. M. McBride, B. K. Weaver, C. Dingwall, and N. C. Reich. 2000. Regulated nuclear-cytoplasmic localization of interferon regulatory factor 3, a subunit of double-stranded RNA-activated factor 1. *Mol. Cell. Biol.* 20: 4159–4168.
36. Yang, H., C. H. Lin, G. Ma, M. O. Baffi, and M. G. Wathelet. 2003. Interferon regulatory factor-7 synergizes with other transcription factors through multiple interactions with p300/CBP coactivators. *J. Biol. Chem.* 278: 15495–15504.

37. Kaltenberg, J., L. M. Plum, J. L. Ober-Blöbaum, A. Hönscheid, L. Rink, and H. Haase. 2010. Zinc signals promote IL-2-dependent proliferation of T cells. *Eur. J. Immunol.* 40: 1496–1503.
38. Siewert, E., W. Müller-Esterl, R. Starr, P. C. Heinrich, and F. Schaper. 1999. Different protein turnover of interleukin-6-type cytokine signalling components. *Eur. J. Biochem.* 265: 251–257.
39. Yang, J., and G. R. Stark. 2008. Roles of unphosphorylated STATs in signaling. *Cell Res.* 18: 443–451.
40. Haase, H., and W. Maret. 2003. Intracellular zinc fluctuations modulate protein tyrosine phosphatase activity in insulin/insulin-like growth factor-1 signaling. *Exp. Cell Res.* 291: 289–298.
41. An, H., W. Zhao, J. Hou, Y. Zhang, Y. Xie, Y. Zheng, H. Xu, C. Qian, J. Zhou, Y. Yu, et al. 2006. SHP-2 phosphatase negatively regulates the TRIF adaptor protein-dependent type I interferon and proinflammatory cytokine production. *Immunity* 25: 919–928.
42. Gabhann, J. N., R. Higgs, K. Brennan, W. Thomas, J. E. Damen, N. Ben Larbi, G. Krystal, and C. A. Jefferies. 2010. Absence of SHIP-1 results in constitutive phosphorylation of tank-binding kinase 1 and enhanced TLR3-dependent IFN-beta production. *J. Immunol.* 184: 2314–2320.
43. Xu, H., H. An, J. Hou, C. Han, P. Wang, Y. Yu, and X. Cao. 2008. Phosphatase PTP1B negatively regulates MyD88- and TRIF-dependent proinflammatory cytokine and type I interferon production in TLR-triggered macrophages. *Mol. Immunol.* 45: 3545–3552.
44. Wilson, M., C. Hogstrand, and W. Maret. 2012. Picomolar concentrations of free zinc(II) ions regulate receptor protein-tyrosine phosphatase β activity. *J. Biol. Chem.* 287: 9322–9326.
45. Kröncke, K. D., and L. O. Klotz. 2009. Zinc fingers as biologic redox switches? *Antioxid. Redox Signal.* 11: 1015–1027.
46. Cotto-Rios, X. M., M. Békés, J. Chapman, B. Ueberheide, and T. T. Huang. 2012. Deubiquitinases as a signaling target of oxidative stress. *Cell Rep* 2: 1475–1484.
47. Kitamura, H., H. Morikawa, H. Kamon, M. Iguchi, S. Hojyo, T. Fukada, S. Yamashita, T. Kaisho, S. Akira, M. Murakami, and T. Hirano. 2006. Toll-like receptor-mediated regulation of zinc homeostasis influences dendritic cell function. *Nat. Immunol.* 7: 971–977.
48. Kawai, T., and S. Akira. 2010. The role of pattern-recognition receptors in innate immunity: update on Toll-like receptors. *Nat. Immunol.* 11: 373–384.
49. MacMicking, J., Q. W. Xie, and C. Nathan. 1997. Nitric oxide and macrophage function. *Annu. Rev. Immunol.* 15: 323–350.